Published in final edited form as:
Clin Cancer Res. 2011 April 1; 17(7): 1815–1827. doi:10.1158/1078-0432.CCR-10-2120.

Vandetanib Restores Head and Neck Squamous Cell Carcinoma Cells' Sensitivity to Cisplatin and Radiation *In Vivo* and *In Vitro*

Daisuke Sano[1], **Fumihiko Matsumoto**[2], **David R. Valdecanas**[2], **Mei Zhao**[1], **David P. Molkentine**[2], **Yoko Takahashi**[1], **Ehab Y. Hanna**[1], **Vali Papadimitrakopoulou**[3], **John Heymach**[3], **Luka Milas**[2], and **Jeffrey N. Myers**[1,4]

[1]Department of Head and Neck Surgery, The University of Texas MD Anderson Cancer Center, Houston, Texas

[2]Department of Experimental Radiation Oncology, The University of Texas MD Anderson Cancer Center, Houston, Texas

[3]Department of Thoracic and Head and Neck Medical Oncology, The University of Texas MD Anderson Cancer Center, Houston, Texas

[4]Department of Cancer Biology, The University of Texas MD Anderson Cancer Center, Houston, Texas

Abstract

Purpose—We investigated whether vandetanib, an inhibitor of the tyrosine kinase activities of vascular endothelial growth factor receptor-2 (VEGFR-2), epidermal growth factor receptor (EGFR) and Rearranged during transfection (RET), could augment the antitumor activity of radiation with or without cisplatin in preclinical *in vitro* and *in vivo* models of human head and neck squamous cell carcinoma (HNSCC).

Experimental design—OSC-19 and HN5 HNSCC cells that were cisplatin and radioresistant were treated with vandetanib, cisplatin, and radiation alone or in combination *in vitro* and *in vivo* using an orthotopic nude mouse model. Treatment effects were assessed using clonogenic survival assay, tumor volume, bioluminescence imaging, tumor growth delay, survival, microvessel density, tumor and endothelial cell apoptosis, and EGFR and Akt phosphorylation data.

Results—Vandetanib plus cisplatin radiosensitized HNSCC cells *in vitro* and *in vivo*. The combination treatment with vandetanib, cisplatin, and radiation was superior to the rest of treatments (including the double combinations) in antitumoral effects, prolonging survival, decreasing cervical lymph node metastases *in vivo*. It also increased both tumor and tumor-associated endothelial cell apoptosis and decreased microvessel density *in vivo*. An analysis of tumor growth delay data revealed that vandetanib plus cisplatin enhanced radioresponse *in vivo*. All vandetanib-containing treatments inhibited EGFR and Akt phosphorylation *in vitro* and *in vivo*.

Conclusion—The addition of vandetanib to combination therapy with cisplatin and radiation was able to effectively overcome cisplatin and radioresistance in *in vitro* and *in vivo* models of HNSCC. Further study of this regimen in clinical trials may be warranted.

Corresponding Author: Jeffrey N. Myers, Department of Head and Neck Surgery, Unit 441, The University of Texas MD Anderson Cancer Center, 1515 Holcombe Boulevard, Houston, TX 77030. Tel: 713-745-2667; Fax: 713-794-4662; jmyers@mdanderson.org.

Keywords

head and neck squamous cell carcinoma; radioresistance; vandetanib; cisplatin; epidermal growth factor receptor (EGFR)

INTRODUCTION

Head and neck squamous cell carcinomas (HNSCC), which represent approximately 3.2% of cancers in the United States, accounted for approximately 49,260 new cancer diagnoses and 11,480 deaths in 2010 (1). Despite advances in treatment, the 5-year survival of patients with HNSCC has not significantly improved over the past several decades (2). Treatment failure primarily takes the form of locoregional recurrences or distant metastatic disease (3).

Although surgery and radiation have traditionally been used to treat locoregionally advanced HNSCC (4), the addition of platinum-based chemotherapy such as cisplatin is playing an increasingly prominent role in HNSCC treatment (5). Treating patients who have locoregionally advanced HNSCC with platinum-based chemotherapy and concurrent radiation improves locoregional control, organ preservation, and disease-free and overall survival (6–8). However, because some patients develop chemo- and radioresistance, only 50–60% of the HNSCC patients treated with radiation and concurrent platinum-based chemotherapy are cured of their disease. To improve treatment efficacy in patients with HNSCC, researchers must have a more thorough understanding of the pathways mediating chemo- and radioresistance (9,10).

Identifying the factors that cause tumor cells' radioresistance is essential to improving therapy outcomes in patients with HNSCC (11). One potential mechanism by which tumor cells become radioresistant is epidermal growth factor receptor (EGFR) signaling, which can be activated by radiation (12). EGFR is overexpressed in a variety of epithelial malignancies including HNSCC (13), and studies have shown that EGFR expression is related to tumor radioresistance (14,15). EGFR overexpression, which occurs in a large portion of HNSCCs, is related to HNSCC growth and development (16) and is predictive of poor prognosis (17). Therefore, inhibiting the EGFR pathway is a potential radiosensitization strategy in patients with HNSCC.

Another potential strategy for overcoming radioresistance in HNSCC is angiogenesis inhibition. In addition to preventing the formation of new blood vessels and interrupting the supply of oxygen and nutrients in tumors (18), anti-angiogenesis therapy alone or in combination with other treatments transiently normalizes the structure and function of tumor vasculature (19). Thus, anti-angiogenic agents could be used to induce a remodeling of the tumor vasculature, leading to a temporary improvement in tumor perfusion and reoxygenation that potentially enhance the actions of chemo- and radiotherapy (20). In addition, anti-angiogenic agents have been reported to enhance the tumor cell response to platinum-based chemotherapeutic drugs (21). Vandetanib (AstraZeneca, Macclesfield, Cheshire, UK), an inhibitor of vascular endothelial growth factor receptor-2 (VEGFR-2), EGFR and Rearranged during Transfection (RET) tyrosine kinases, has the potential to restore chemo- and radiosensitivity of HNSCC cells.

In a previous study, we found that vandetanib alone and in combination with paclitaxel had beneficial therapeutic effects in an orthotopic mouse model of human HNSCC (22). However, the combination of vandetanib, radiation, and current chemotherapeutic agents used for HNSCC treatment has not yet been evaluated preclinically. We investigated

whether vandetanib could augment the antitumor activity of cisplatin with or without concurrent radiation in preclinical *in vitro* and *in vivo* models of human HNSCC.

MATERIALS AND METHODS

Animals

We purchased 8-to-12-week-old male athymic nude mice from the National Cancer Institute (Bethesda, MD). The mice were kept in a specific pathogen–free facility approved by the American Association for the Accreditation of Laboratory Animal Care that met all current regulations and standards of the U.S. Department of Agriculture, U.S. Department of Health and Human Services, and the National Institutes of Health. Mice were fed irradiated standard mouse chow and autoclaved, reverse osmosis–treated water. Animal procedures were carried out according to a protocol approved by The University of Texas MD Anderson Cancer Center's Institutional Animal Care and Use Committee.

Cell lines

Seventeen human HNSCC cell lines were used. FaDu cells were obtained from American Type Culture Collection (Manassas, VA). Dr. Luka Milas provided HN5 cells. UM-SCC-1, -4, -11A, -14A, -17A, -17B, -22A, and -47 cells were provided by Dr. Thomas Carey (Department of Otolaryngology/Head and Neck Surgery, University of Michigan). TU-138 cells were provided by Dr. Gary Clayman (Department of Head and Neck Surgery, MD Anderson Cancer Center). SCC-61 cells were provided by Dr. Ralph Weichselbaum (Department of Radiation and Cellular Oncology, University of Chicago). OSC-19 cells were obtained from Dr. Faye Johnson (Department of Thoracic/Head and Neck Medical Oncology, MD Anderson Cancer Center). SqCC/Y1 cells were obtained from Dr. Vali Papadimitrakopoulou. MDA-1386TU cells were obtained from Dr. Peter G. Sacks (Department of Basic Sciences, New York University). TR-146 cells were provided by Dr. Ho-Young Lee (Department of Thoracic/Head and Neck Medical Oncology, MD Anderson Cancer Center). PCI-13 cells were provided by Dr. Jennifer Grandis, (Department of Otolaryngology, The University of Pittsburgh Medical Center).

OSC-19 cells were retrovirally infected with the green fluorescent protein and the luciferase gene (OSC-19-luc) as described previously (23). SCC61 cells were maintained in Dulbecco's modified Eagle's medium (DMEM) supplemented with 20% fetal bovine serum (FBS), L-glutamine, sodium pyruvate, nonessential amino acids, a 2-fold vitamin solution (Life Technologies, Inc., Grand Island, NY), and 0.4 μg/mL hydrocortisone. SqCC/Y1 cells were maintained in DMEM/F12 low glucose supplemented with 10% FBS and L-glutamine. JHU028 cells were maintained in RPMI 1640 supplemented with 10% FBS, L-glutamine, sodium pyruvate, and nonessential amino acids. All other HNSCC cells were maintained in DMEM supplemented with 10% FBS, L-glutamine, sodium pyruvate, nonessential amino acids, and a 2-fold vitamin solution. Adherent monolayer cultures were maintained on plastic plates and incubated at 37°C in 5% carbon dioxide and 95% oxygen. The cultures were *Mycoplasma*-free and maintained for no longer than 12 weeks after they were recovered from frozen stocks.

Reagents

Vandetanib (ZD6474) was provided by AstraZeneca Pharmaceuticals (Macclesfield, Cheshire, UK). For *in vivo* testing, vandetanib was dissolved in phosphate-buffered saline (PBS) containing 1% Tween 80. For *in vitro* testing, stock solutions of vandetanib were prepared in dimethylsulfoxide (Sigma-Aldrich Corp., St. Louis, MO) and diluted with culture medium. Cisplatin was purchased from Sigma-Aldrich as a stock solution of 1 mg/mL. For animal studies, cisplatin was diluted in 0.9% saline immediately before injection.

Propidium iodide and 3-(4,5-dimethylthiazol-2-yl)-2,5-diphenyl-tetrazolium bromide (MTT) were purchased from Sigma-Aldrich. Stock solutions were prepared by dissolving either 0.5 mg of propidium iodide or 2 mg of MTT in 1 mL of PBS. Each solution was filtered, protected from light, stored at 4°C, and used within 1 month.

Rat monoclonal anti-mouse CD31 (platelet-endothelial cell adhesion molecule 1; PECAM), the primary antibody for immunohistochemical analysis, was purchased from BD Pharmingen (San Diego, CA). The secondary antibodies, peroxidase-conjugated goat anti-rat immunoglobulin G1 and Alexa Fluor 594-conjugated goat anti-rat immunoglobulin G, were purchased from Jackson Research Laboratories (West Grove, PA) and Invitrogen (Carlsbad, CA), respectively.

Cell proliferation assay

The antiproliferative activity of cisplatin against HNSCC cells *in vitro* was determined using an MTT assay as previously described (24). Briefly, 17 HNSCC cell lines were plated in 96-well plates in medium. After a 24-h attachment period, the cells were incubated for 72 h in various concentrations of cisplatin (0.01–90 μM) or with PBS alone as a control. Cells were then incubated in medium containing 2% FBS and 0.25 mg/mL MTT for 3 h. The cells were then lysed in 100 mL dimethylsulfoxide to release formazan. We used an EL-808 96-well plate reader (BioTek Instruments, Winooski, VT) set at an absorbance of 570 nm to quantify the conversion of MTT to formazan. The concentration of vandetanib giving 50% growth inhibition (GI50) for each cell line was calculated using GraphPad Prism 5.01 (GraphPad Software, San Diego, CA). The experiment was repeated at least twice. The vandetanib GI50 was the average of the values from each MTT assay.

Clonogenic survival assay

To determine the sensitivity of the 17 HNSCC cell lines to radiation, we performed a clonogenic survival assay. Cells in culture were exposed to 2, 4, or 6 Gy radiation (γ-rays using a cesium-137 source, 3.055 Gy/min). The cells were then assayed for colony-forming ability by trypsinizing and replating specified numbers of cells in 100-mm dishes in drug-free medium. After 10–12 d of incubation, the cells were stained with 0.5% crystal violet in absolute ethanol, and colonies with more than 50 cells were counted under a dissection microscope.

OSC-19 and HN5 cells were used in further studies, since they were both cisplatin and radiation-resistant, according to results from MTT assay and clonogenic survival assay with 17 HNSCC cell lines. OSC-19 and HN5 cells in culture were exposed to cisplatin (4 μM and 9 μM, respectively) for 1 h, exposed to vandetanib (2 μM and 2.5 μM, respectively) for 6 h, and then irradiated. After treatments, the cells were assayed for colony-forming ability as described above. Plating efficiency was defined as the percentage of cells seeded that grow into colonies under a specific culture condition of a given cell line. The survival fraction, expressed as a function of irradiation, was calculated as the number of colonies counted/(the number of cells seeded×plating efficiency/100). The surviving fraction after 2 Gy (SF2) was used to determine the radiation sensitivity.

Orthotopic nude mouse model of HNSCC

We used an orthotopic nude mouse model of HNSCC because its host microenvironment is more similar to that of patients with HNSCC than that of subcutaneous xenograft models of HNSCC (25). OSC-19-luc, OSC-19, and HN5 cells were harvested from subconfluent cultures by trypsinization and washed with PBS. An orthotopic nude mouse model of an oral tongue tumor was established by injecting OSC-19-luc (1×10^5), OSC-19 (1×10^5), or HN5

(2×10^5) cells suspended in 30 μL of serum-free DMEM into the tongues of mice as described previously (26).

Eight to 10 d after the cells were injected, the mice were randomly assigned to 1 of 8 treatment groups (7 or 8 mice per group): (1) control; (2) cisplatin; (3) vandetanib; (4) vandetanib plus cisplatin; (5) radiation; (6) cisplatin plus radiation; (7) vandetanib plus radiation; (8) vandetanib plus cisplatin and radiation. Cisplatin was administered intravenously once a week for 2 weeks at a dose of 1 mg/kg, and vandetanib was administered by oral gavage once a day for 2 weeks at a dose of 20 mg/kg. Control mice were given 200 μL of 1% Tween 80 by oral gavage once daily for 2 weeks and/or 200 μL PBS intraperitoneally once weekly for 2 weeks.

Mice bearing tumors in the tongue were locally irradiated with a single dose of 5 Gy using a small-animal irradiator (γ-rays using a cesium-137 source, 4.762 Gy/min). Sodium pentobarbital was administered by intraperitoneal injection at a dose of 50 mg/kg prior to radiation treatment. The mice were immobilized on a customized jig during irradiation with the tumor centered in the 3-cm diameter circular irradiation field. When cisplatin and radiation were combined, cisplatin was given 1 h before single-dose irradiation (27). When vandetanib and radiation were combined, vandetanib was given 4 h before single-dose irradiation (28).

Mice were examined twice a week for tumor size and weight loss. Tongue tumor size was measured with microcalipers. Tumor volume was calculated as $(A)(B^2)\pi/6$, where A is the longest dimension of the tumor and B is the dimension of the tumor perpendicular to A. The degree of growth delay was expressed as the absolute tumor growth delay (AGD), defined as the time in days required for OSC-19-luc tumors HN5 tumors to grow to 40 mm^3 minus the time in days for the tumors in the untreated control group to reach the same sizes; or the normalized growth delay (NGD), defined as the time in d required for OSC-19-luc tumors and HN5 tumors to grow to 40 mm^3 minus the time to reach the same size in mice treated with drug (s) alone. Treatment enhancement factors (EFs) were obtained by dividing the NGD in mice treated with drugs plus radiation by the AGD in mice treated with radiation alone (29).

We used bioluminescence imaging to monitor orthotopic tumor growth *in vivo*. Bioluminescence was quantified using Living Image software 3.2 (Xenogen, Alameda, CA) as described previously (30). Animals were anesthetized with 2% isoflurane (Abbott, Abbott Park, IL), and an aqueous solution of luciferin (Xenogen) at 150 mg/kg in a volume of 0.1 mL was injected intraperitoneally 5 min prior to imaging. We used an IVIS 200 Imaging System (Xenogen) to image the animals and Living Image software (Xenogen) to quantify the photons emitted from luciferase-expressing cells. Photon flux was calculated using a rectangular region of interest encompassing the head and neck region of each mouse while in a dorsal position. Animals were imaged on an almost weekly basis. Before engineered OSC-19-luc cells were used *in vivo*, we used the IVIS imaging system to confirm *in vitro* that the cells homogeneously expressed high levels of luciferase.

We euthanized mice by CO_2 asphyxiation when they lost more than 20% of their preinjection body weight or at 50 d after cell injection. Half of the mouse tumors were fixed in formalin and embedded in paraffin for immunohistochemical and hematoxylin-and-eosin staining; the other half were embedded in optimal cutting temperature compound (Miles, Inc., Elkhart, IN), rapidly frozen in liquid nitrogen, and stored at −80°C. Cervical lymph nodes were resected, embedded in paraffin, sectioned, stained with hematoxylin and eosin. The presence of cervical lymph node metastasis was evaluated histologically using one H&E slide which was from a paraffin block prepared for each animal.

Immunohistochemical analysis and immunofluorescence double staining analysis for CD31–terminal deoxynucleotidyl transferase-mediated deoxyuridine triphosphate nick-end labeling

Frozen tissues were immunohistochemically and immunofluorescently analyzed. Slide preparation and immunostaining for CD31/PECAM-1 were performed as previously described (24). We performed terminal deoxynucleotidyl transferase-mediated deoxyuridine triphosphate nick-end labeling (TUNEL) assay with a DeadEnd Fluorometric TUNEL System (Promega, Madison, WI). Samples were fixed with 4% paraformaldehyde for 10 min, washed twice with PBS for 5 min, and then incubated with 0.2% Triton X-100 for 15 min. After two 5-min washes with PBS, the samples were incubated with equilibration buffer for 10 min. The equilibration buffer was drained, and reaction buffer (44 μL equilibration buffer, 5 μL nucleotide mix, and 1 μL TDT) was added to the samples. The samples were then incubated in a humid atmosphere at 37°C for 1 h in the dark. The reaction was terminated by immersing the samples in 2× standard saline citrate for 15 min. Samples were then washed with PBS to remove unincorporated fluorescein-dUTP. For CD31-TUNEL double staining, the samples were fixed with acetone, washed with PBS, incubated with protein-blocking solution containing 5% normal horse serum and 1% normal goat serum in PBS for 20 min, and then incubated in a 1:400 dilution of anti-CD31/PECAM-1 antibody for 1 h. The samples were then washed with PBS and incubated in a 1:600 dilution of a secondary antibody conjugated with Alexa Fluor 594 for 1 h in the dark. For CD31-TUNEL double staining, the samples were then sequentially stained in the TUNEL assay.

Immunofluorescence microscopy was performed using a Leica DMLA microscope (Leica Microsystems, Bannockburn, IL) equipped with a 100-watt HBO mercury bulb and filter sets (Chroma, Inc., Brattleboro, VT) to reveal red and blue fluorescent images independently. Images were captured using a cooled charge-coupled Hamamatsu C5810 camera (Hamamatsu Corp., Bridgewater, NJ) and ImagePro Plus 6.0 software (Media Cybernetics, Silver Spring, MD). Photomontages were prepared using Adobe Photoshop 10.0.1 software (Adobe Systems, Inc., San Jose, CA).

Quantification of microvessel density and apoptotic endothelial cells

To quantify TUNEL expression, we counted the positively stained cells in 10 random 0.04-mm^2 fields at ×200 magnification per slide. To quantify microvessel density (MVD), we identified areas containing high numbers of tumor-associated blood vessels at ×100 magnification; vessels that had stained completely with anti-CD31 antibody were counted in 12 random 0.04-mm^2 fields at ×200 magnification. We calculated the number of apoptotic endothelial cells as the average of the ratio of apoptotic endothelial cells to the total number of endothelial cells in 10 random 0.04-mm^2 fields at ×400 magnification.

Western blotting

Western blot analyses of tumor and cultured cells were performed. Tumors were snap-frozen in liquid nitrogen and homogenized in lysis buffer. OSC-19 cells (2×10^5 per well) were plated in 6-well plates (Costar, Cambridge, MA) in 2 mL medium containing 10% FBS, incubated for 24 h, and then treated with vandetanib, cisplatin, and irradiation as described above. Total cell lysates were then obtained and subjected to Western blot analysis as previously described (24). The membranes were blocked for 1 h at room temperature with 5% bovine serum albumin in 0.1% Tween 20 in Tris-buffered saline and incubated overnight at 4°C with anti-EGFR (Santa Cruz Biotechnology, Santa Cruz, CA; 1:500), anti-phospho-EGFR (Tyr^{1068}; Cell signaling, Beverly, MA; 1:500), anti-Akt (Cell signaling; 1:1000), anti-phospho-Akt (Ser^{473}; Cell signaling; 1:1000), anti–mitogen-activated protein kinase (MAPK; Cell signaling; 1:1000), or anti-phospho-MAPK (Thr^{202}/Try^{204}; Cell signaling; 1:1000) in 5% bovine serum albumin in 0.1% Tween 20 in Tris-buffered saline.

Next, the membranes were washed with 0.1% Tween 20 in Tris-buffered saline and incubated for 1 h at room temperature in horseradish peroxidase–conjugated anti-rabbit immunoglobulin G (Santa Cruz Biotechnology, Santa Cruz, CA) to detect EGFR, phosphorylated EGFR, or species-appropriate fluorescently conjugated proteins (goat anti-rabbit IRDye 800 and goat anti-mouse IRDye 800, Invitrogen). The membranes were then analyzed using the SuperSignal West chemiluminescent system (Pierce Biotechnology, Rockford, IL) and an Odyssey Infrared Imaging System (LI-COR Biosciences, Lincoln, NE), and relevant signal intensities were determined using LI-COR imaging software 3.0. To verify equal protein loading, we stripped and reprobed the membranes with anti-β-actin (1:5000).

Statistical analysis

Potential correlations between SF2 and cisplatin GI50 values were analyzed by the Pearson's correlation coefficients with *P* values for the two-tailed test of significance. Two-tailed *t* tests were used to compare tumor volumes between control groups and treatment groups. Survival was determined using the Kaplan-Meier method and compared using log-rank tests. Fisher's exact test was used to analyze associations between treatment groups and cervical lymph node metastases. Quantitative data related to the immunohistochemical expression of CD31 and CD31-TUNEL were compared with two-tailed Student's *t* tests. Statistical analyses were performed with Prism 5.01 software (GraphPad Software). *P* values < 0.05 were considered statistically significant.

RESULTS

OSC-19 HNSCC cells and HN5 HNSCC cells were cisplatin- and radiation-resistant

MTT assays with cisplatin and clonogenic survival assays with radiation revealed cisplatin GI50 values ranging from 1.03 μM to 9.52μM and SF2 values ranging from 0.22 to 0.80 (Supplementary Table S1). SF2 values were not correleated with cisplatin GI50 values ($R=0.0992$, $P=0.4132$, data not shown). OSC-19 cells and HN5 cells were relatively cisplatin and radiation-resistant: The cisplatin GI50 values were 5.19 μM for OSC-19 cells and 9.08 μM for HN5 cells, and the SF2 values were 0.63 for OSC-19 cells and 0.70 for HN5 cells (Supplementary Table S1).

Vandetanib plus cisplatin radiosensitized OSC-19 and HN5 cells

In clonogenic survival assays, radiation alone resulted in a dose-dependent decrease in HN5 and OSC-19 cell survival. Cell growth inhibition was observed in both cell lines after 1 h of exposure to cisplatin and 6 h of exposure to vandetanib. OSC-19 cells treated with 2 μM vandetanib and 4 μM cisplatin exhibited more growth inhibition than control cells (Fig. 1A). While the radiosensitizing effect of treatment with 2.5 μM vandetanib and 9 μM cisplatin on HN5 cells was milder than the radiosensitizing effect on OSC-19, both cell lines demonstrated enhancement compared with control cells (Fig. 1B).

Vandetanib plus cisplatin and radiation inhibits both human radiation- resistance and cisplatin & radiation-resistance HNSCC tumor growth in an orthotopic nude mouse model

In the OSC-19 model, there was a significant antitumor effect in the mice treated with vandetanib plus cisplatin and radiation compared with the mice in the control group on day 35 after cell inoculation ($P = 0.0106$; Fig. 2A). Mice in the cisplatin alone group, vandetanib alone group, radiation alone group, cisplatin plus radiation group, and vandetanib plus radiation group all had smaller tumor volumes than mice in the control group; however, the difference was not statistically significant. In addition, the vandetanib plus cisplatin and radiation group also showed significant antitumor effect compared with the vandetanib alone

group, cisplatin alone group, radiation alone group, and the vandetanib plus radiation group ($P = 0.0059$, $P = 0.0039$, $P = 0.0051$, and $P = 0.0366$, respectively). To see the effects of the treatment, we also monitored the bioluminescence intensity of OSC-19-luc cells (Fig. 2C and 2F). The mice treated with vandetanib plus cisplatin and radiation had a marked reduction in bioluminescence compared to mice in the control group on day 32 significantly ($P = 0.0006$).

The antitumor effects of treatment with the combination treatment with vandetanib plus cisplatin, and radiation were also observed in the HN5 orthotopic model (Fig. 2B). The mice treated with vandetanib, cisplatin, and radiation had a significantly lower mean tumor volume than the mice in the control group at day 35 ($P < 0.0001$). A significant antitumor effect was also observed in the mice treated with vandetanib alone ($P = 0.0076$), vandetanib plus cisplatin ($P < 0.0001$) and the mice treated with vandetanib plus radiation ($P = 0.0001$). The mice treated with vandetanib, cisplatin, and radiation also had a significantly lower mean tumor volume than the mice in the cisplatin alone group and the cisplatin plus radiation group ($P = 0.0002$ and $P = 0.0451$, respectively). The antitumor effects of these treatments were confirmed in a repeat animal experiment with OSC-19 and HN5 cells (data not shown). All treatments appeared to be well-tolerated, with no evidence of treatment-related weight loss (data not shown).

Vandetanib plus cisplatin enhanced the radiosensitivity of orthotopic HNSCC tumors

The antitumor effects of the experimental treatments measured by tumor growth delay are shown in Table 1. Cisplatin only slightly delayed tumor growth by 2.9 ± 0.9 d, and a single dose of 5 Gy radiation delayed tumor growth by 5.1 ± 1.1 d, whereas vandetanib treatment delayed tumor growth by 10.6 ± 0.8 d. When vandetanib and cisplatin were combined, the AGD value (11.3 ± 1.0 d) was smaller than the sum of tumor growth delays caused by individual treatments (EF = 0.23).

Cisplatin plus radiation slowed tumor growth more than additively; the treatment increased AGD to 10.5 ± 3.1 d (EF = 1.50). However, vandetanib plus radiation only slightly increased AGD to 13.4 ± 1.2 d (EF = 0.55). In contrast, vandetanib plus cisplatin and radiation achieved a more than additive effect, resulting in an AGD of 25.6 ± 4.0 d, which was considerably higher than the sum of tumor growth delays caused by individual treatments (5.1 ± 1.1 d with radiation and 11.3 ± 1.0 d with vandetanib plus cisplatin; EF = 2.82).

Similarly, while cisplatin enhanced the effects of radiation treatment in HN5 tumors (EF = 1.62), the addition of vandetanib treatment to radiation only slightly increased AGD (EF = 0.45). However, vandetanib plus cisplatin enhanced the radioresponsiveness of HN5 tumors, increasing tumor growth delay more than additively even though 2 of 8 mice which were cured were not used in the analysis (EF = 1.42/data not shown). Thus, vandetanib plus cisplatin enhanced HNSCC tumors' radioresponse more than vandetanib plus radiation.

Vandetanib plus cisplatin and radiation prolonged survival in an orthotopic nude mouse model of human HNSCC

All OSC-19-luc control mice in the survival study were euthanized within 25 days following cell inoculation (Fig. 2D). The median survival duration for the control mice was 19.5 d. The median survival periods for the cisplatin, vandetanib, vandetanib plus cisplatin, radiation, cisplatin plus radiation, vandetanib plus radiation, and vandetanib plus cisplatin and radiation groups in the OSC-19-luc mice were 24.5 ($P = 0.0396$), 30.5 ($P < 0.0001$), 30.0 ($P < 0.0001$), 27.0 ($P = 0.0041$), 35.0 ($P < 0.0001$), 34.0 ($P = 0.0002$), and 42.5 d ($P < 0.0001$), respectively (P vs. controls). The median survival period for the vandetanib plus

cisplatin and radiation group was significantly greater when compared to that for the cisplatin alone group, vandetanib alone group, vandetanib plus cisplatin group, radiation alone group, and vandetanib plus radiation group ($P = 0.0003$, $P < 0.0001$, $P = 0.0007$, $P = 0.0003$, and $P = 0.0140$, respectively).

All HN5 control mice in the survival study were euthanized within 38 days following cell inoculation (Fig. 2E). The median survival period for the control group was 31.0 d. The median survival periods for the cisplatin, vandetanib, vandetanib plus cisplatin, radiation, cisplatin plus radiation, vandetanib plus radiation, and vandetanib plus cisplatin and radiation groups in the HN5 mice were 28.0 ($P = 0.3931$), 50.0 ($P = 0.0008$), 50.0 ($P = 0.0002$), 42.0 ($P = 0.0111$), 50.0 ($P = 0.0008$), 50.0 ($P = 0.0002$), and 50.0 d ($P < 0.0001$), respectively (P vs. controls). The median survival period for the vandetanib plus cisplatin and radiation group was also significantly longer compared to that for the cisplatin alone group and the radiation alone group ($P = 0.0002$, and $P = 0.0036$, respectively).

Vandetanib, alone or in combination with cisplatin and radiation, reduced the incidence of cervical lymph node metastases in an orthotopic nude mouse model of HNSCC

In the mice with OSC-19 tumors, cervical lymph node metastases were detected in 75.0% of control mice, 66.7% of cisplatin-treated mice, 58.3% of vandetanib-treated mice, 58.3% of vandetanib and cisplatin–treated mice, 61.5% of radiation-treated mice, 53.8% of cisplatin and radiation–treated mice, 46.2% of vandetanib plus radiation–treated mice, and 15.3% of vandetanib plus cisplatin and radiation–treated mice (Table 2). Thus, combination treatment markedly inhibited the development of cervical lymph node metastases, and the difference in cervical lymph node metastasis incidence between mice treated with vandetanib, cisplatin, and radiation and control mice was significant ($P = 0.0048$). In addition, the vandetanib, cisplatin, and radiation group showed decreased cervical lymph node metastases when compared to the cisplatin alone group, vandetanib alone group, radiation alone group, and the vandetanib plus cisplatin group ($P = 0.0154$, $P = 0.0414$, $P = 0.0414$, $P = 0.0414$, respectively). The difference between the control group and any another treatment group did not reach statistical significance.

In the mice with HN5 tumors, 40.0% of control mice, 11.1% of cisplatin-treated mice, 27.2% of radiation-treated mice, and 18.1% of cisplatin and radiation–treated mice had cervical lymph node metastases. No cervical lymph node metastases were found in vandetanib-treated mice, vandetanib and cisplatin–treated mice, vandetanib and radiation–treated mice, or vandetanib, cisplatin, and radiation–treated mice (Table 2) and the difference for all treatment groups compared to the control group was significant ($P < 0.05$).

Vandetanib with or without cisplatin increased tumor endothelial cell apoptosis and decreased MVD *in vivo* in OSC-19 xenografts

Immunostaining tumor sections with CD31 antibody showed that the MVD of tumors from mice treated with vandetanib (31.00 ± 3.32; $P < 0.0001$), vandetanib plus cisplatin (29.92 ± 2.18; $P < 0.0001$), cisplatin plus radiation (43.42 ± 3.17; $P = 0.0118$), vandetanib plus radiation (24.08 ± 1.59; $P < 0.0001$) or vandetanib plus cisplatin and radiation (12.75 ± 1.92; $P < 0.0001$) was significantly lower than that of tumors in control mice (55.75 ± 3.18; Fig. 3A and B). The MVD of tumors in the vandetanib plus cisplatin and radiation was also significantly lower than that in the other treatment groups ($P < 0.001$).

TUNEL assay was performed to examine cell apoptosis *in vivo*. Compared to the percentage of TUNEL-positive cells in the tumors from mice in the control group ($0.92\% \pm 0.29\%$), the percentages of TUNEL-positive cells in the tumors from mice in all treatment groups were increased significantly (cisplatin, $3.72\% \pm 0.85\%$; vandetanib, $11.49\% \pm 0.67\%$; vandetanib

plus cisplatin, 12.46% ± 1.22%; radiation, 9.98% ± 1.09%; cisplatin plus radiation, 16.58% ± 2.03%; vandetanib plus radiation, 19.03% ± 2.99%; vandetanib plus cisplatin and radiation, 24.41% ± 2.50%). The difference for all treatment groups compared to the control group was significant (P <0.01)(Fig. 3A and 3C). In addition, the percentages of TUNEL-positive cells in the vandetanib plus cisplatin and radation group were also significantly greater than in the vandetanib alone group, cisplatin alone group, radiation alone group, and the vandetanib plus radiation group (P <0.05).

Double immunofluorescence staining for CD31/TUNEL revealed that vandetanib, vandetanib plus cisplatin, and vandetanib plus radiation significantly increased apoptosis for tumor-associated endothelial cells compared to the control group (control, 0%; vandetanib, 5.38 ± 2.51, P =0.0460; vandetanib plus cisplatin, 5.62 ± 2.40, P =0.0306; vandetanib plus radiation, 5.94 ± 2.53, P =0.0304). The apoptosis for tumor-associated endothelial cells was further enhanced when vandetanib was combined with radiation and cisplatin (8.01 ± 2.74; P = 0.0090) (Fig. 3A and 3D).

Vandetanib with or without cisplatin and/or radiation inhibited epidermal growth factor receptor and Akt phosphorylation *in vitro* and *in vivo*

Western blot analysis of orthotopic OSC-19 xenograft tumours was performed to confirm that the vandetanib-containing treatments inhibited the phosphorylation of EGFR and its downstream targets, Akt and MAPK. In OSC-19 tumors, pY1068 EGFR was inhibited by treatment with vandetanib alone, vandetanib plus cisplatin, vandetanib plus radiation, and vandetanib plus cisplatin and radiation after 7 d (Fig. 4A). We also found that the vandetanib-containing treatments inhibited Akt and MAPK phosphorylation in OSC-19 tumors; however, treatment did not inhibit Akt phosphorylation in some of the tumors in mice in the vandetanib alone, vandetanib plus cisplatin, and vandetanib plus radiation groups. These *in vivo* results confirmed *in vitro* findings with Western blot analysis of OSC-19 cells that vandetanib alone or in combination with cisplatin and/or radiation inhibited EGFR phosphorylation (Fig. 4B).

DISCUSSION

We found that vandetanib augmented the antitumor activity of cisplatin with concurrent radiation in preclinical models of human cisplatin- and radiation-resistant HNSCC *in vitro* and *in vivo*. Vandetanib plus cisplatin effectively radiosensitized HNSCC cells both *in vitro* and *in vivo*. Vandetanib alone or in combination with cisplatin and/or radiation inhibited the phosphorylation of EGFR and its downstream mediators, Akt and MAPK, both *in vitro* and *in vivo*. Treatment with vandetanib, cisplatin, and radiation led to reductions in tumor size and cervical lymph node metastases and prolonged survival in an orthotopic nude mouse model by inducing apoptosis in tumor and endothelial cells.

Chemoradiotherapy with cisplatin remains a standard treatment for patients with HNSCC, with the aim of improving organ preservation as well as patient survival (31). However, resistance to cisplatin or radiation leading to treatment failure and locoregional recurrence is a critical problem. In addition, cisplatin causes significant treatment-limiting toxicities including such as myelosuppression, nephrotoxicity, ototoxicity and nephrotoxicity, which can be exacerbated by radiotherapy (8,32). Therefore, the addition of more selective agents that target cancer cells may enable the reduction of cisplatin and possibly radiation to less toxic doses.

A number of studies have shown that the EGFR and its downstream PI3K pathway mediate radio-resistance (14,15,33). In a phase III randomized trial, Bonner et al. found that patients with locally advanced HNSCC who were treated with radiation plus cetuximab, a

monoclonal antibody against EGFR, had better locoregional control, longer disease-free survival, and longer overall survival than patients treated with radiation alone (34). In addition, anti-angiogenic agents have been reported to enhance radioresponsiveness (35). These previous studies indicate a potentially important role for EGFR and VEGFR signaling in radio-resistance and suggest that blocking these receptors may result in improved response to radiotherapy. Therefore, we evaluated whether the combination of cisplatin and radiotherapy with vandetanib, a potent inhibitor of both VEGFR and EGFR signaling, may represent a valuable therapeutic approach against experimental HNSCC cancer in this study.

In the present study, OSC-19 and HN5 were selected as representative cell lines as relatively cisplatin- and radiation-resistant cell lines from a panel of 17 different HNSCC cell lines. In this study we found a lack of correlation between radiosensitivity and cisplatin sensitivity consistent with the results of previous reports (36,37). The effect of cisplatin on radiosensitization on HN5 was weaker than on OSC-19, which is consistent with the GI50 values for cisplatin alone. In the current study, although 1 mg/kg of cisplatin had only a slight antitumor effect, treatment with cisplatin and radiation slowed OSC-19-luc and HN5 tumor growth more than additively. These results are consistent with those of previous studies that led to the widespread use of cisplatin as a radiosensitizer (38).

In the current study, vandetanib slowed tumor growth to a greater extent than cisplatin alone. Mice treated with vandetanib had significantly longer survival than control mice. These results are consistent with the results of our previous study (22). However, in our previous study, we found that the GI50 of vandetanib for HN5 cells (2.357) was higher than its GI50 for OSC-19 cells (1.981) (22), whereas in the current study, we found no significant differences in the antitumor effects of vandetanib *in vivo* between HN5 tumors and OSC-19-luc tumors. This inconsistency may have arisen because vandetanib's antitumor effects in HNSCC may be a result of the agent's inhibition of VEGF signaling within the tumor microvasculature rather than its direct antiproliferative effects via EGFR signaling inhibition. These inconsistent findings might also reflect the biological differences between the two cell lines. When vandetanib was combined with radiation, it did not significantly enhance the response of OSC-19-luc or HN5 tumors to radiation. However, a number of studies have shown that vandetanib enhances radiation effects in preclinical models (28,39,40) including HNSCC (41). This inconsistency may have been due to the relatively low dose of vandetanib (20 mg/kg) used in the current study, differences in vandetanib and/or radiation treatment schedules, and differences in the type of preclinical mouse models used. However, the combined treatment with vandetanib, cisplatin and radiation showed the most marked reduction in OSC-19-luc and HN5 tumor growth and prolongation of survival in orthotopic oral tongue tumor models compared with not only control but also when compared to all of the other treatments. Similar results with significant tumor inhibition by the combination of vandetanib, cytotoxic chemotherapy and radiation have been reported for other xenograft tumor models (42,43).

Although vandetanib given with low concentrations of cisplatin has been reported to have synergistic activity in bladder cancer (21), the addition of cisplatin to vandetanib treatment in our *in vivo* studies showed only a slight additive effect. Ansiaux et al. reported that the blockade of of VEGFR signaling reduces oxygen consumption rate in tumor cells and cause an early increase in tumor oxygenation (44). Thus, the mechanism by which treatment with vandetanib plus cisplatin and radiation exerted its antitumor effect could be the result of a short-term increase in blood flow and oxygenation in the tumor, leading to improved delivery of cisplatin, which led to more cisplatin-induced radiosensitization in the current study.

The presence of cervical lymph node metastasis is a critical event for patients with HNSCC (3). In the current study, treatment with vandetanib alone inhibited metastases in HN5 mice; however, cisplatin and/or radiation did not significantly decrease the incidence of cervical lymph node metastases. While the difference was not significant, OSC-19 mice treated with vandetanib alone and OSC-19 mice treated with vandetanib plus radiation had a much lower incidence of cervical lymph node metastases than control mice. These findings are consistent with our previous reports in which the blockade of both EGFR and VEGFR-2 pathways decreased the incidence of the neck lymph node metastases of HNSCC (22,30). Moreover, treatment with vandetanib, cisplatin, and radiation produced the most marked decrease in cervical lymph node metastasis incidence.

In the present study, immunohistochemical analysis and TUNEL assay revealed that vandetanib significantly decreased tumor MVD and induced apoptosis in tumor and endothelial cells. These findings are consistent with the results of our previous study as well as other studies (22,28,39,40). Slight decreases in MVD along with enhanced radiation-induced endothelial apoptosis is consistent with a previous report indicating that radiation can kill tumor cells as well as tumor-associated endothelial cells (45). Again, the combined treatment with vandetanib, cisplatin and radiation showed the most marked induction of apoptosis in tumor and endothelial cells, and suppression of MVD compared with the other treatment groups, indicating that vandetanib enhanced the combined effect of cisplatin and radiation. Finally, we confirmed previous studies' findings that the inclusion of vandetanib leads to inhibition of EGFR activation and its downstream radioresistance-mediating signaling pathways in oral tongue tumors (14,15). Although the inclusion of vandetanib into the treatment schedules inhibited EGFR and MAPK phosphorylation in OSC-19 oral tongue tumors, phosphorylation was not inhibited in some tumors treated with vandetanib, vandetanib plus cisplatin, and vandetanib plus radiation. This may have been attributable to predominance of the anti-angiogenic activity of vandetanib compared to the blockade of EGFR signaling. Indeed, vandetanib's primary antitumor effect in tumor endothelial cells is believed to be generated by its inhibition of VEGFR signaling (46).

Several clinical trials of vandetanib plus cytotoxic chemotherapy and/or radiation are currently under way (http://clinicaltrials.gov/ct2/results?term=vandetanib). For HNSCC, clinical trials of EGFR-inhibiting agents combined with cisplatin have shown that these treatments are active and well tolerated meriting additional investigation (47–49). Papadimitrakopoulou et al. reported that 100 mg of vandetanib was the maximum tolerated dose when it was combined with radiation and cisplatin in patients with previously untreated advanced HNSCC (50).

In conclusion, we found that vandetanib plus cisplatin enhanced HNSCC radioresponsiveness *in vitro* and *in vivo* and that vandetanib plus cisplatin, and radiation had significant antitumor activity in an orthotopic mouse model of HNSCC and inhibited cervical lymph node metastases *in vivo*. The combination treatment with vandetanib, cisplatin, and radiation induced apoptosis in endothelial and tumor cells, decreased tumor MVD, and blocked EGFR phosphorylation to help to overcome radioresistance in HNSCC. These results suggest that vandetanib sensitizes some HNSCC cells to cisplatin and radiation. This combined treatment could have potential as treatment against advanced HNSCC and may warrant further evaluation in clinical trials.

Statement of Translational Relevance

While chemoradiotherapy with platinum compounds is one of the standard treatment regimens for patients with head and neck squamous cell carcinoma (HNSCC), some HNSCCs are resistant and persist/recur after this type of treatment. In this study, we

showed vandetanib, an inhibitor of vascular endothelial growth factor receptor-2 (VEGFR-2), epidermal growth factor receptor (EGFR) and Rearranged during Transfection (RET) tyrosine kinases, plus cisplatin radiosensitized both HNSCC cells *in vitro* and *in vivo*. Vandetanib in combination with cisplatin and radiation inhibited both tumor growth and the incidence of cervical lymph node metastases, and prolonged survival in an orthotopic nude mouse model of HNSCC. Thus, the blockade of both VEGFR-2 and EGFR pathway by the addition of vandetanib to combination therapy with cisplatin and radiation may overcome cisplatin- and radioresistance in HNSCC effectively and this regimen could represent a potential novel therapeutic strategy that may warrant evaluation for patients with advanced HNSCC.

Supplementary Material

Refer to Web version on PubMed Central for supplementary material.

Acknowledgments

We thank Joseph A. Munch for his critical editorial review of the manuscript.

Grant Support: This work was supported by AstraZeneca, The University of Texas MD Anderson Cancer Center's PANTHEON program, NIH Specialized Program of Research Excellence Grant P50CA097007, National Research Science Award Institutional Research Training Grant T32CA60374, and NIH Cancer Center Support (Core) Grant CA016672.

REFERENCES

1. Jemal A, Siegel R, Xu J, Ward E. Cancer Statistics, 2010. CA Cancer J Clin. 2010
2. Goldberg HI, Lockwood SA, Wyatt SW, Crossett LS. Trends and differentials in mortality from cancers of the oral cavity and pharynx in the United States, 1973–1987. Cancer. 1994; 74:565–572. [PubMed: 8033034]
3. Sano D, Myers JN. Metastasis of squamous cell carcinoma of the oral tongue. Cancer Metastasis Rev. 2007; 26:645–662. [PubMed: 17768600]
4. Forastiere AA. Is there a new role for induction chemotherapy in the treatment of head and neck cancer? J Natl Cancer Inst. 2004; 96:1647–1649. [PubMed: 15547172]
5. Adelstein DJ, Li Y, Adams GL, et al. An intergroup phase III comparison of standard radiation therapy and two schedules of concurrent chemoradiotherapy in patients with unresectable squamous cell head and neck cancer. J Clin Oncol. 2003; 21:92–98. [PubMed: 12506176]
6. Brizel DM, Albers ME, Fisher SR, et al. Hyperfractionated irradiation with or without concurrent chemotherapy for locally advanced head and neck cancer. N Engl J Med. 1998; 338:1798–1804. [PubMed: 9632446]
7. Forastiere AA, Goepfert H, Maor M, et al. Concurrent chemotherapy and radiotherapy for organ preservation in advanced laryngeal cancer. N Engl J Med. 2003; 349:2091–2098. [PubMed: 14645636]
8. Cooper JS, Pajak TF, Forastiere AA, et al. Postoperative concurrent radiotherapy and chemotherapy for high-risk squamous-cell carcinoma of the head and neck. N Engl J Med. 2004; 350:1937–1944. [PubMed: 15128893]
9. Gibson MK, Li Y, Murphy B, et al. Randomized phase III evaluation of cisplatin plus fluorouracil versus cisplatin plus paclitaxel in advanced head and neck cancer (E1395): an intergroup trial of the Eastern Cooperative Oncology Group. J Clin Oncol. 2005; 23:3562–3567. [PubMed: 15908667]
10. Rabbani A, Hinerman RW, Schmalfuss IM, et al. Radiotherapy and concomitant intraarterial cisplatin (RADPLAT) for advanced squamous cell carcinomas of the head and neck. Am J Clin Oncol. 2007; 30:283–286. [PubMed: 17551306]
11. West CM, Davidson SE, Roberts SA, Hunter RD. Intrinsic radiosensitivity and prediction of patient response to radiotherapy for carcinoma of the cervix. Br J Cancer. 1993; 68:819–823. [PubMed: 8398714]

12. Dent P, Reardon DB, Park JS, et al. Radiation-induced release of transforming growth factor alpha activates the epidermal growth factor receptor and mitogen-activated protein kinase pathway in carcinoma cells, leading to increased proliferation and protection from radiation-induced cell death. Mol Biol Cell. 1999; 10:2493–2506. [PubMed: 10436007]
13. Mendelsohn J, Baselga J. The EGF receptor family as targets for cancer therapy. Oncogene. 2000; 19:6550–6565. [PubMed: 11426640]
14. Gupta AK, McKenna WG, Weber CN, et al. Local recurrence in head and neck cancer: relationship to radiation resistance and signal transduction. Clin Cancer Res. 2002; 8:885–892. [PubMed: 11895923]
15. Liang K, Ang KK, Milas L, Hunter N, Fan Z. The epidermal growth factor receptor mediates radioresistance. Int J Radiat Oncol Biol Phys. 2003; 57:246–254. [PubMed: 12909240]
16. Shin DM, Ro JY, Hong WK, Hittelman WN. Dysregulation of epidermal growth factor receptor expression in premalignant lesions during head and neck tumorigenes. Cancer Res. 1994; 54:3153–3159. [PubMed: 8205534]
17. Ang KK, Berkey BA, Tu X, et al. Impact of epidermal growth factor receptor expression on survival and pattern of relapse in patients with advanced head and neck carcinoma. Cancer Res. 2002; 62:7350–7356. [PubMed: 12499279]
18. Folkman J. Role of angiogenesis in tumor growth and metastasis. Semin Oncol. 2002; 29:15–18. [PubMed: 12516034]
19. Jain RK. Normalization of tumor vasculature: an emerging concept in antiangiogenic therapy. Science. 2005; 307:58–62. [PubMed: 15637262]
20. Jain RK. Normalizing tumor vasculature with anti-angiogenic therapy: a new paradigm for combination therapy. Nat Med. 2001; 7:987–989. [PubMed: 11533692]
21. Flaig TW, Su LJ, McCoach C, et al. Dual epidermal growth factor receptor and vascular endothelial growth factor receptor inhibition with vandetanib sensitizes bladder cancer cells to cisplatin in a dose- and sequence-dependent manner. BJU Int. 2009; 103:1729–1737. [PubMed: 19220256]
22. Sano D, Fooshee DR, Zhao M, et al. Targeted molecular therapy of head and neck squamous cell carcinoma with the tyrosine kinase inhibitor vandetanib in a mouse model. Head Neck. 2010 Jul 13. [Epub ahead of print].
23. Zhou G, Xie TX, Zhao M, et al. Reciprocal negative regulation between S100A7/psoriasin and beta-catenin signaling plays an important role in tumor progression of squamous cell carcinoma of oral cavity. Oncogene. 2008; 27:3527–3538. [PubMed: 18223693]
24. Yigitbasi OG, Younes MN, Doan D, et al. Tumor cell and endothelial cell therapy of oral cancer by dual tyrosine kinase receptor blockade. Cancer Res. 2004; 64:7977–7984. [PubMed: 15520205]
25. Sano D, Myers JN. Xenograft models of head and neck cancers. Head Neck Oncol. 2009; 1:32. [PubMed: 19678942]
26. Myers JN, Holsinger FC, Jasser SA, Bekele BN, Fidler IJ. An orthotopic nude mouse model of oral tongue squamous cell carcinoma. Clin Cancer Res. 2002; 8:293–298. [PubMed: 11801572]
27. McNally LR, Rosenthal EL, Zhang W, Buchsbaum DJ. Therapy of head and neck squamous cell carcinoma with replicative adenovirus expressing tissue inhibitor of metalloproteinase-2 and chemoradiation. Cancer Gene Ther. 2009; 16:246–255. [PubMed: 18846112]
28. Shibuya K, Komaki R, Shintani T, et al. Targeted therapy against VEGFR and EGFR with ZD6474 enhances the therapeutic efficacy of irradiation in an orthotopic model of human non-small-cell lung cancer. Int J Radiat Oncol Biol Phys. 2007; 69:1534–1543. [PubMed: 17889445]
29. Milas L, Fujii T, Hunter N, et al. Enhancement of tumor radioresponse in vivo by gemcitabine. Cancer Res. 1999; 59:107–114. [PubMed: 9892194]
30. Sano D, Choi S, Milas ZL, et al. The effect of combination anti-endothelial growth factor receptor and anti-vascular endothelial growth factor receptor 2 targeted therapy on lymph node metastasis: a study in an orthotopic nude mouse model of squamous cell carcinoma of the oral tongue. Arch Otolaryngol Head Neck Surg. 2009; 135:411–420. [PubMed: 19380367]
31. Ang KK, Harris J, Garden AS, et al. Concomitant boost radiation plus concurrent cisplatin for advanced head and neck carcinomas: radiation therapy oncology group phase II trial 99-14. J Clin Oncol. 2005; 23:3008–3015. [PubMed: 15860857]

32. Garden AS, Asper JA, Morrison WH, et al. Is concurrent chemoradiation the treatment of choice for all patients with Stage III or IV head and neck carcinoma? Cancer. 2004; 100:1171–1178. [PubMed: 15022283]
33. Schuurbiers OC, Kaanders JH, van der Heijden HF, Dekhuijzen RP, Oyen WJ, Bussink J. The PI3-K/AKT-pathway and radiation resistance mechanisms in non-small cell lung cancer. J Thorac Oncol. 2009; 4:761–767. [PubMed: 19404218]
34. Bonner JA, Harari PM, Giralt J, et al. Radiotherapy plus cetuximab for squamous-cell carcinoma of the head and neck. N Engl J Med. 2006; 354:567–578. [PubMed: 16467544]
35. O'Reilly MS. Radiation combined with antiangiogenic and antivascular agents. Semin Radiat Oncol. 2006; 16:45–50. [PubMed: 16378906]
36. Kato T, Duffey DC, Ondrey FG, et al. Cisplatin and radiation sensitivity in human head and neck squamous carcinomas are independently modulated by glutathione and transcription factor NF-kappaB. Head Neck. 2000; 22:748–759. [PubMed: 11084634]
37. Tanaka T, Yukawa K, Umesaki N. Radiation enhances cisplatin-sensitivity in human cervical squamous cancer cells in vitro. Eur J Gynaecol Oncol. 2005; 26:431–433. [PubMed: 16122195]
38. Douple EB. Platinum-radiation interactions. NCI Monogr. 1988:315–319. [PubMed: 3352776]
39. Brazelle WD, Shi W, Siemann DW. VEGF-associated tyrosine kinase inhibition increases the tumor response to single and fractionated dose radiotherapy. Int J Radiat Oncol Biol Phys. 2006; 65:836–841. [PubMed: 16751064]
40. Wu W, Onn A, Isobe T, et al. Targeted therapy of orthotopic human lung cancer by combined vascular endothelial growth factor and epidermal growth factor receptor signaling blockade. Mol Cancer Ther. 2007; 6:471–483. [PubMed: 17308046]
41. Gustafson DL, Frederick B, Merz AL, Raben D. Dose scheduling of the dual VEGFR and EGFR tyrosine kinase inhibitor vandetanib (ZD6474, Zactima) in combination with radiotherapy in EGFR-positive and EGFR-null human head and neck tumor xenografts. Cancer Chemother Pharmacol. 2008; 61:179–188. [PubMed: 17393165]
42. Bianco C, Giovannetti E, Ciardiello F, et al. Synergistic antitumor activity of ZD6474, an inhibitor of vascular endothelial growth factor receptor and epidermal growth factor receptor signaling, with gemcitabine and ionizing radiation against pancreatic cancer. Clin Cancer Res. 2006; 12:7099–7107. [PubMed: 17145834]
43. Wachsberger P, Burd R, Ryan A, Daskalakis C, Dicker AP. Combination of vandetanib, radiotherapy, and irinotecan in the LoVo human colorectal cancer xenograft model. Int J Radiat Oncol Biol Phys. 2009; 75:854–861. [PubMed: 19801101]
44. Ansiaux R, Dewever J, Gregoire V, Feron O, Jordan BF, Gallez B. Decrease in tumor cell oxygen consumption after treatment with vandetanib (ZACTIMA; ZD6474) and its effect on response to radiotherapy. Radiat Res. 2009; 172:584–591. [PubMed: 19883226]
45. Garcia-Barros M, Paris F, Cordon-Cardo C, et al. Tumor response to radiotherapy regulated by endothelial cell apoptosis. Science. 2003; 300:1155–1159. [PubMed: 12750523]
46. Wedge SR, Ogilvie DJ, Dukes M, et al. ZD6474 inhibits vascular endothelial growth factor signaling, angiogenesis, and tumor growth following oral administration. Cancer Res. 2002; 62:4645–4655. [PubMed: 12183421]
47. Chen C, Kane M, Song J, et al. Phase I trial of gefitinib in combination with radiation or chemoradiation for patients with locally advanced squamous cell head and neck cancer. J Clin Oncol. 2007; 25:4880–4886. [PubMed: 17971583]
48. Kuhnt T, Sandner A, Wendt T, et al. Phase I trial of dose-escalated cisplatin with concomitant cetuximab and hyperfractionated-accelerated radiotherapy in locally advanced squamous cell carcinoma of the head and neck. Ann Oncol. 21:2284–2289. [PubMed: 20427347]
49. Rivera F, Garcia-Castano A, Vega N, Vega-Villegas ME, Gutierrez-Sanz L. Cetuximab in metastatic or recurrent head and neck cancer: the EXTREME trial. Expert Rev Anticancer Ther. 2009; 9:1421–1428. [PubMed: 19828002]
50. Papadimitrakopoulou V, Frank SJ, Blumenschein GR, et al. Phase I evaluation of vandetanib with radiation therapy (RT) ± cisplatin in previously untreated advanced head and neck squamous cell carcinoma (HNSCC). J Clin Oncol. 2009; 27 abstr 6016.

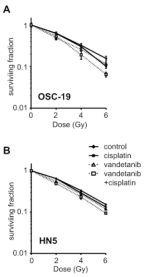

Figure 1.

Effects of vandetanib and/or cisplatin on radiosensitivity of head and neck squamous cell carcinoma cells. OSC-19 and HN5 cells in culture were exposed to cisplatin (4 μM and 9 μM, respectively) for 1 h, vandetanib (2 μM and 2.5 μM, respectively) for 6 h and then irradiated at 2 Gy, 4 Gy, or 6 Gy. After treatments, clonogenic survival assays were performed. Points indicate the means of triplicate experiments; bars, standard errors.

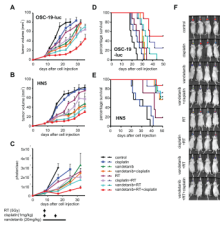

Figure 2.

In vivo effects of treatment with radiation, vandetanib, cisplatin, and their combinations on tumor growth, bioluminescence imaging, and survival time in mice. A, The *in vivo* effects of treatments on tumor growth in OSC-19-luc mice. B, The *in vivo* effects of treatments on tumor growth in HN5 mice. OSC-19-luc and HN5 human HNSCC cells were injected into the tongues of nude mice. After tumor nodules had developed, mice were treated. Tumors were measured with microcalipers twice a week. Points indicate means; bars, standard errors. C, The effects of treatment on OSC-19-luc orthotopic tumor followed by bioluminescence imaging. Points, mean; bars, SE. Photon counts were calculated from the imaging data using the IVIS Living Image software. D, The *in vivo* effects of treatments on survival time in OSC-19 mice. E, The *in vivo* effects of treatments on survival time in HN5 mice. Animals were euthanized when they had lost more than 20% of their initial body weight or at 50 d after cell inoculation. Survival was analyzed by the Kaplan-Meier method and compared with log-rank tests. F, Representative bioluminescence images corresponding to OSC-19-luc tumors from each treatment group, 17 days after cell inoculation.

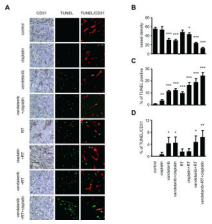

Figure 3.
Immunohistochemical analyses of OSC-19 xenograft tumors in nude mice. A, Tumors were harvested after 7 d of treatment, and representative sections obtained from OSC-19 tumors were immunostained for expression of CD31 (endothelial cell marker) and TUNEL (tumor cell apoptosis) (magnification × 200). Double staining for CD31 (red)/TUNEL (green) was also performed to reveal apoptosis in tumor-associated endothelial cells (magnification × 400). Results of quantitative analysis for B, CD31 staining (microvessel density); C, TUNEL staining; and D, endothelial cells apoptosis. Columns indicate means; bars, standard errors; *, $P < 0.05$; **, $P < 0.01$ as compared with controls; ***, $P < 0.001$ as compared with controls.

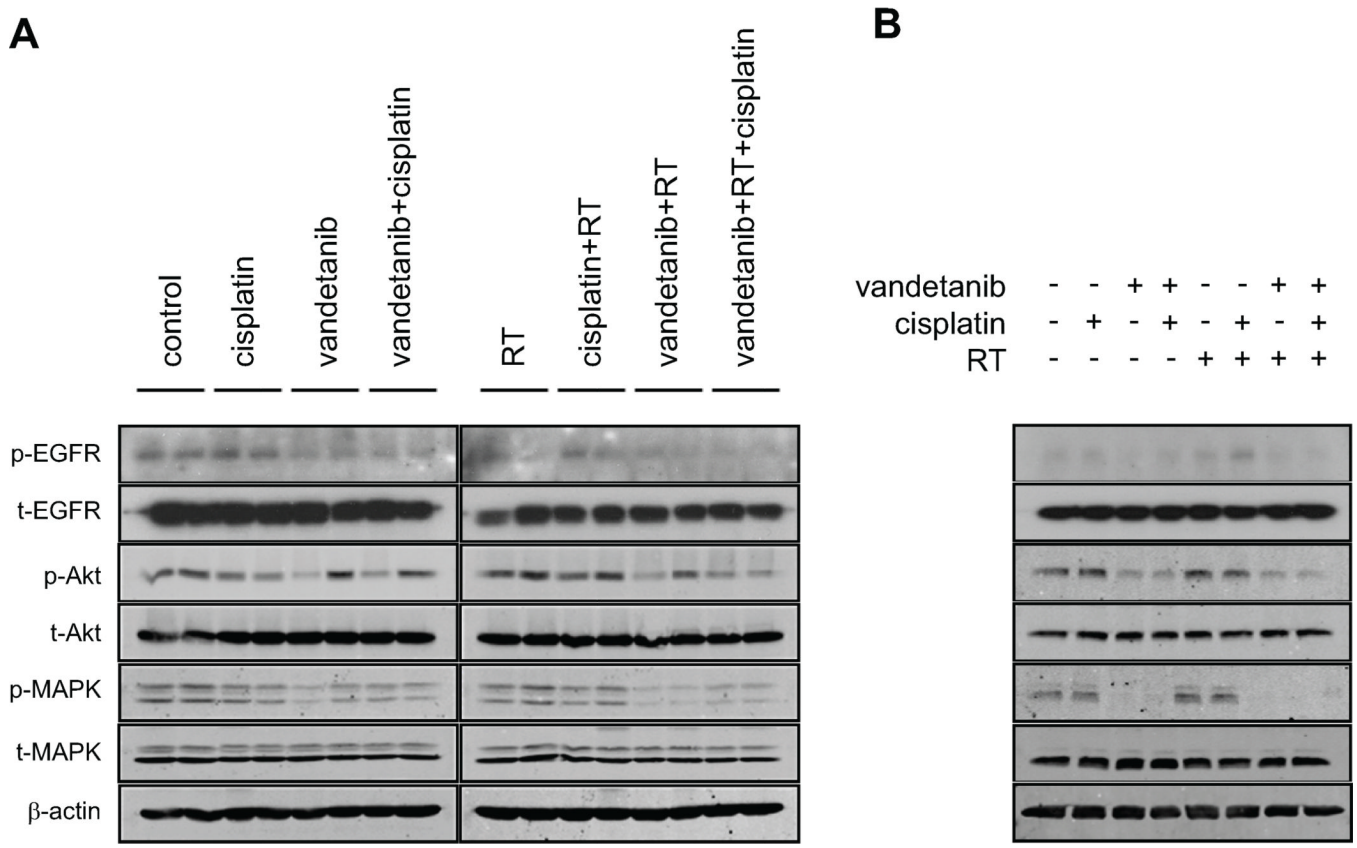

Figure 4.

Vandetanib alone or in combination with cisplatin and/or radiation inhibited epidermal growth factor receptor and Akt phosphorylation *in vivo* and *in vitro* (OSC-19). A, Tumors were harvested after 7 d of treatment, and snap-frozen in liquid nitrogen. They were then homogenized in lysis buffer before being subjected to Western immunoblotting. B, Cells were treated with 2 μM of vandetanib for 6 h, 4 μM of cisplatin for 1 h, and irradiation (3 Gy). Whole-cell lysates were obtained and subjected to Western immunoblotting to resolve proteins. Antibodies to total (unphosphorylated) receptors and β-actin were used as protein loading controls.

Table 1

Effect of treatment on human head and neck squamous cell carcinoma cells' radioresponse.

Treatment	Time required to grow to 40 mm^3, d	Absolute growth delay, d	Normalized growth delay, d	Enhancement factor
Control	13.8 ± 0.6			
Cisplatin	16.8 ± 0.9	2.9 ± 0.9		
Vandetanib	24.5 ± 0.8	10.6 ± 0.8		
Vandetanib+cisplatin	25.1 ± 1.0	11.3 ± 1.0	0.7 ± 1.0 *	0.23 †
Radiation	18.9 ± 1.1	5.1 ± 1.1		
Cisplatin+radiation	24.4 ± 3.1	10.5 ± 3.1	7.6 ± 3.1 ¶	1.50 §
Vandetanib+radiation	27.2 ± 1.2	13.4 ± 1.2	2.8 ± 1.2 ¶	0.55 §
Vandetanib+radiation+cisplatin	39.4 ± 4.0	25.6 ± 4.0	14.3 ± 4.0 ‡	2.82 §

NOTE: All data are means ± standard error unless otherwise indicated.

* Defined as the time in days for tumors to reach 40 mm^3 in the mice treated with the combination of vandetanib and cisplatin, minus the time in days to reach 40 mm^3 in mice treated with vandetanib alone

† Obtained by dividing normalized tumor growth delay in mice treated with vandetanib and cisplatin with the absolute growth delay in mice treated with cisplatin alone.

¶ Defined as the time in days for tumors to reach 40 mm^3 in the mice treated with the combination of vandetanib or cisplatin plus radiation, minus the time in days to reach 40 mm^3 in mice treated with vandetanib or cisplatin alone.

‡ Defined as the time in days for tumors to reach 40 mm^3 in the mice treated with the combination of vandetanib and cisplatin plus radiation, minus the time in days to reach 40 mm^3 in mice treated with vandetanib plus cisplatin.

§ Obtained by dividing normalized tumor growth delay in mice treated with vandetanib or cisplatin plus radiation, or vandetanib, cisplatin plus radiation with the absolute growth delay in mice treated with radiation alone.

Table 2

Effects of treatment with vandetanib, cisplatin, and radiation, alone or in combination, on lymph node metastases in nude mice bearing orthotopic head and neck squamous cell carcinoma xenografts.

Treatment	OSC-19 xenografts		HN5 xenografts	
	Mice with cervical lymphatic metastasis, %	Fisher's exact test vs. control	Mice with cervical lymphatic metastasis, %	Fisher's exact test vs. control
Control	75.0		40.0	
Cisplatin	66.7	0.9999	11.1	0.3034
Vandetanib	58.3	0.6668	0.00	0.0350
Vandetanib+cisplatin	58.3	0.6668	0.00	0.0350
Radiation	61.5	0.6727	27.2	0.6594
Cisplatin+radiation	53.8	0.4109	18.1	0.3614
Vandetanib+radiation	46.2	0.2261	0.00	0.0287
Vandetanib+radiation+cisplatin	15.3	0.0048	0.00	0.0350